Original article

Nuclear Medicine Communications

Breast-specific gamma imaging with Tc-99m-sestamibi in the diagnosis of breast cancer and its semiquantitative index correlation with tumor biologic markers, subtypes, and clinicopathologic characteristics

Hui Tan[a,d,e,*], Hongwei Zhang[b,*], Weige Yang[b,*], Yipeng Fu[b], Yusen Gu[a,d,e], Min Du[c], Dengfeng Cheng[a,d,e] and Hongcheng Shi[a,d,e]

Objectives **To determine the sensitivity of breast-specific gamma imaging (BSGI) in diagnosing breast cancer and assess the potential correlation between the semiquantitative index of BSGI and biologic markers, molecular subtypes, and clinicopathologic characteristics of breast cancer.**

Materials and methods **The sensitivity of BSGI for breast cancer was retrospectively assessed in 102 female breast cancer patients who underwent BSGI before surgery and was compared with that of ultrasonography and mammography. BSGI was visually graded on the basis of the Society of Nuclear Medicine and Molecular Imaging guideline. Tracer uptake in the cancer as the lesion to nonlesion ratio (L/N) was calculated semiquantitatively and was subsequently correlated to tumor biologic markers, molecular subtypes, and clinicopathologic characteristics.**

Results **The sensitivity of BSGI for breast cancer by visual analysis was 94.1% (96/102) in our cohort, which was 100% (47/47) in the subgroup of patients with a tumor size more than 2.0 cm and 89.1% (49/55) in the subgroup of patients with a size less than or equal to 2.0 cm. The sensitivity of BSGI was significantly higher than that of ultrasonography of 84.2% (85/101) ($P = 0.022$) and mammography of 84.5% (60/71) ($P = 0.037$). There was no significant correlation between the L/N and expressions of estrogen receptor, progesterone receptor, human epidermal growth factor receptor 2, and antigen Ki-67, and the subtypes or histologic grade of the cancer ($P > 0.05$). However, the value of L/N was associated with infiltration degree ($P = 0.005$), axillary lymph node status ($P = 0.029$), and tumor size ($P = 0.002$). Multivariate analysis further indicated that the value of L/N was correlated with infiltration degree ($P = 0.016$) and tumor size ($P = 0.002$).**

Conclusion **BSGI has a high sensitivity for detecting primary breast cancer. The value of L/N on BSGI was independently related to infiltration degree and tumor size of breast cancer, but not to expression of tumor receptor markers and histologic grade.** ***Nucl Med Commun*** **37:792–799**

Nuclear Medicine Communications 2016, **37**:792–799

Keywords: biologic markers, breast cancer, breast-specific gamma imaging, clinicopathologic factors, sensitivity, Tc-99m-sestamibi

Departments of [a]Nuclear Medicine, [b]General Surgery, [c]Pathology, Zhongshan Hospital, Fudan University, [d]Nuclear Medicine Institute of Fudan University and [e]Shanghai Institute of Medical Imaging, Shanghai, China

Correspondence to Hongcheng Shi, MD, PhD, Department of Nuclear Medicine, Zhongshan Hospital, Fudan University, Shanghai 200032, China
Tel/fax: +86 21 64041990 2064;
e-mail: shi.hongcheng@zs-hospital.sh.cn

*Hui Tan, Hongwei Zhang and Weige Yang contributed equally to the writing of this article.

Received 21 December 2015 **Revised** 13 February 2016
Accepted 15 March 2016

Introduction

Breast cancer is the most common malignancy in women. Mammography (MMG) and ultrasonography (US) are frequently used anatomic imaging tools to screen and diagnose breast cancer. However, there are limitations for both the MMG and the US in detection of breast cancer. The sensitivity of 78–85% for MMG in diagnosing breast cancer decreases to 30–48% in patients with dense breast tissues [1,2]. US is operator dependent, and has a high false-positive rate with a low specificity [3,4]. Nuclear medicine techniques such as technetium-99m sestamibi (Tc-99m-MIBI) scintimammography provide a unique complementary diagnosis tool for functional imaging. Compared with Tc-99m-MIBI scintimammography, breast-specific gamma imaging (BSGI) has a higher resolution, with a smaller field of view. It has been used widely in recent years for diagnosing breast cancer, especially in the context of dense breasts, scars, and implants [5–7].

Breast cancer pathophysiology is complex because of its marked heterogeneity, with distinct molecular characteristics and subtypes, with different managements accordingly. Several factors including tumor size, histologic grade, axillary lymph node status, biologic markers [including estrogen receptor (ER), progesterone receptor (PR) and human epidermal growth factor receptor 2 (Her-2) status, and antigen Ki-67 (Ki-67)], and molecular subtypes have been shown to be able to predict the biologic behavior as well as the prognosis of breast cancer [8–11].

DOI: 10.1097/MNM.0000000000000518

Studies have shown that uptake of Tc-99m-MIBI in scintimammography was associated with breast cancer tumor size, histologic grade, axillary lymph nodes status, and biologic marker positivity [12,13]. However, little is known about the correlation of Tc-99m-MIBI uptake in BSGI with these features [14] as well as its relation to the varying molecular subtypes of breast cancer.

Therefore, in this study, we evaluated the sensitivity of BSGI in diagnosing breast cancer and compared it with that of US and MMG. In addition, we aimed to determine any independent correlation between the semiquantitative index of lesion to nonlesion ratio (L/N) on BSGI and the expression of biologic markers (ER, PR, Her-2, and Ki-67), molecular subtypes, as well as clinicopathologic characteristics of breast cancer.

Materials and methods

Patients

From March 2012 to October 2013, 178 patients with a breast mass underwent a BSGI examination in our institution. In this study, only a subgroup of patients who had BSGI scans initially with a subsequent pathological diagnosis of primary breast carcinoma were enrolled. Those patients who had been diagnosed with breast cancer by biopsy or fine needle aspiration of breast tissue and axillary lymph nodes, or followed by treatment before BSGI were excluded.

Finally, 102 female patients who had BSGI initially with a subsequent histologic diagnosis of breast cancer were retrospectively analyzed. The mean age of the patients was 57.77 ± 11.73 years (range 31–87 years). This study was approved by the Institutional Review Board of Zhongshan Hospital, Fudan University. Among the 102 patients, 101 patients had US and 71 had digital MMG within 15 days.

Tc-99m-MIBI BSGI

BSGI scan was performed in 10–15 min following an intravenous administration of 740 MBq Tc-99m-MIBI (Shanghai GMS Pharmaceutical Co. Ltd, Shanghai, China) through an antecubital vein contralateral to the suspicious breast side to avoid potential false-positive uptake in the axillary lymph nodes. The patients remained seated during the procedure. Craniocaudal (CC) and mediolateral oblique (MLO) images were obtained in both breasts using a high-resolution BSGI (Dilon 6800; Dilon Technologies, Newport News, Virginia, USA). A low-energy general-purpose collimator was used, with a photopeak focused at 140 keV with a symmetric 10% window. The acquisition time for each image was ~ 6 min, with a value of 100 000 counts per image defined as the minimal range.

Analysis of US and MMG images

US was performed using a Sequ-oia 512 scanner (Siemens, Mountain View, California, USA), an ESAOTEDU-8 scanner (Esaote, Florence, Italy), or an EUB-8500 scanner (Hitachi, Tokyo, Japan) with a 7.5–12 MHz probe. CC and MLO images were obtained of the breasts bilaterally by MMG using a senographe DS (GE Medical Systems, Fairfield, Connecticut, USA). The US and MMG results were interpreted by two experienced ultrasound physicians and radiologists, respectively, who were unaware of the pathology and other examination results. In case of discrepancy, a consensus was reached after mutual discussion. For US and MMG, BI-RADS categories 0–3 were classified as negative and BI-RADS categories 4 and 5 were classified as positive.

Analysis of BSGI images

BSGI images were analyzed by two experienced nuclear medicine physicians who were blinded to the patients' clinical information and pathology results. In cases of discrepancy, a consensus was reached after mutual discussion. According to the 2010 guideline of the Society of Nuclear Medicine and Molecular Imaging [15], visual analysis grades of BSGI were as follows (Fig. 1): grade 1 (homogeneous uptake), grade 2 (small patchy uptake), grade 3 (patchy uptake with mild to moderate intensity), grade 4 (mild focal uptake), and grade 5 (definite focal uptake). A result of grades 4 to 5 was considered to be positive, and grades of 1 to 3 were considered to be negative [6,16].

After visual assessment of BSGI images, a semiquantitative analysis of the L/N was carried out (Fig. 1) [6]. First, a region of interest (ROI) was manually drawn on the lesion area in CC and the same ROI was placed on a nonlesion area, which was approximately equal to the distance between the nonlesion and the lesion area to the nipple. Second, the radioactivity count of the lesion area was divided by the corresponding count of the nonlesion area as the L/N value of CC. The same method was used for the L/N value on an MLO view. The higher L/N value of CC and MLO was selected as the semiquantitative index for analysis.

Immunohistochemical staining

Infiltration degree, histologic grade, tumor size, and axillary lymph node status were determined from the surgically excised specimens. The expressions of ER, PR, Her-2, and Ki-67 were evaluated in the surgically excised specimens using standard avidin–biotin complex immunohistochemical staining techniques. ER and PR positivity were defined as the presence of 1% or more positively stained nuclei in 10 high-power fields [17]. The intensity of Her-2 staining was classified as 0 (no staining), 1+ (weak and incomplete membrane staining), 2+ (strong, complete membrane staining in $\leq 30\%$ of tumor cells or weak/moderate heterogeneous complete staining in $\geq 10\%$ of tumor cells), and 3+ (strong, complete membrane staining in $> 30\%$ of tumor cells). Tumors with a score of 3+ were classified as Her-2 positive those with a score of 0 or 1+ were classified as

Fig. 1

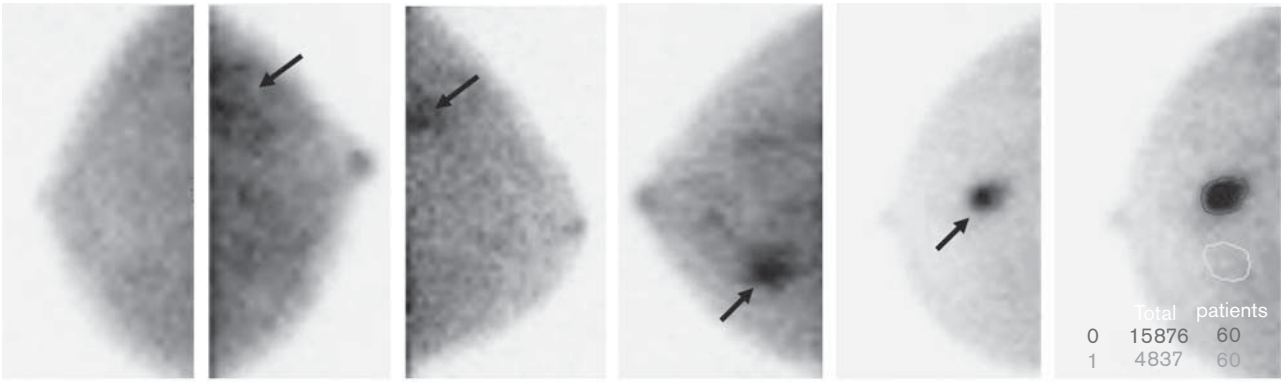

Methods of visual and semiquantitative analysis for BSGI images. BSGI, breast-specific gamma imaging; L/N, lesion to nonlesion ratio. Arrows show the uptake of Tc-99m-MIBI in breast.

Her-2 negative. Gene amplification using fluorescence in-situ hybridization (FISH) was used to determine Her-2 status in tumors with a score of 2+.

Molecular classification

On the basis of the results of immunohistochemical analysis and FISH, the tumors were categorized into four molecular subtypes: luminal A (ER positive and/or PR positive, Her-2 negative, and Ki-67 < 14%), luminal B (ER positive and/or PR positive, Her-2 negative, and Ki-67 ≥ 14%; or ER positive and/or PR positive, Her-2 positive, irrespective of Ki-67 expression), Her-2 positive (ER negative, PR negative, and Her-2 positive), and triple negative or basal (ER negative, PR negative, and Her-2 negative).

Statistical analysis

SPSS, 19.0 software for Windows (SPSS Inc., Chicago, Illinois, USA) was used for statistical analysis, with *P*-values of less than 0.05 indicating a statistically significant difference. Differences in semiquantitative variants were analyzed using Pearson's χ^2-test. The correlations between the L/N and biologic markers, molecular subtypes, and clinicopathologic characteristics of breast cancer were analyzed and compared using Student's *t*-test and multivariate analysis with linear regression.

Results

Pathology

The pathology of breast cancer is shown in Table 1, Figs 2 and 3. Other rare types included malignant phyllodes tumor, Pagets' disease, secretory carcinoma, squamous cell carcinoma, respectively ($n = 1$), and neuroendocrine carcinoma ($n = 2$).

Table 1 Infiltration degree of breast cancer

Type	Cases ($N = 102$) [n (%)]
Infiltrating ductal carcinoma	78 (76.47)
DCIS	13 (12.75)
Infiltrating lobular carcinoma	2 (1.96)
Micropapillary carcinoma	2 (1.96)
Others	7 (6.86)

DCIS, ductal carcinoma *in situ*.

Analysis of BSGI, US, and MMG

Of the 102 breast cancer cases, the sensitivity of BSGI with visual analysis in diagnosing breast cancer was 94.1% (96/102). When the group was stratified by tumor size, the sensitivity was 100% (47/47) for tumor size more than 2.0 cm and 89.1% (49/55) for size less than or equal to 2.0 cm. The corresponding sensitivity of US in diagnosing breast cancer was 84.2% (85/101). Fourteen of 16 misdiagnosed cases by US were identified accurately by BSGI. The sensitivity of MMG in diagnosing breast cancer was 84.5% (60/71). In addition, six cases with dense breast tissue out of the 11 missed breast carcinoma patients by MMG were identified successfully by BSGI. There was a statistically significant difference between BSGI and US ($P = 0.022$) and between BSGI and MMG ($P = 0.037$) for diagnosing breast cancer.

Correlations between the value of L/N and biologic markers

As shown in Table 2, the semiquantitative index of L/N showed no statistically significant correlation with ER, PR, Her-2, and Ki-67 of breast cancers. In addition, the difference was not statistically significant among the Her-2 staining intensity scored 0 and 1+, and 2+ ($t = 1.580$, $P = 0.120$), that scored 0 and 1+, and 3+ ($t = 0.700$,

Fig. 2

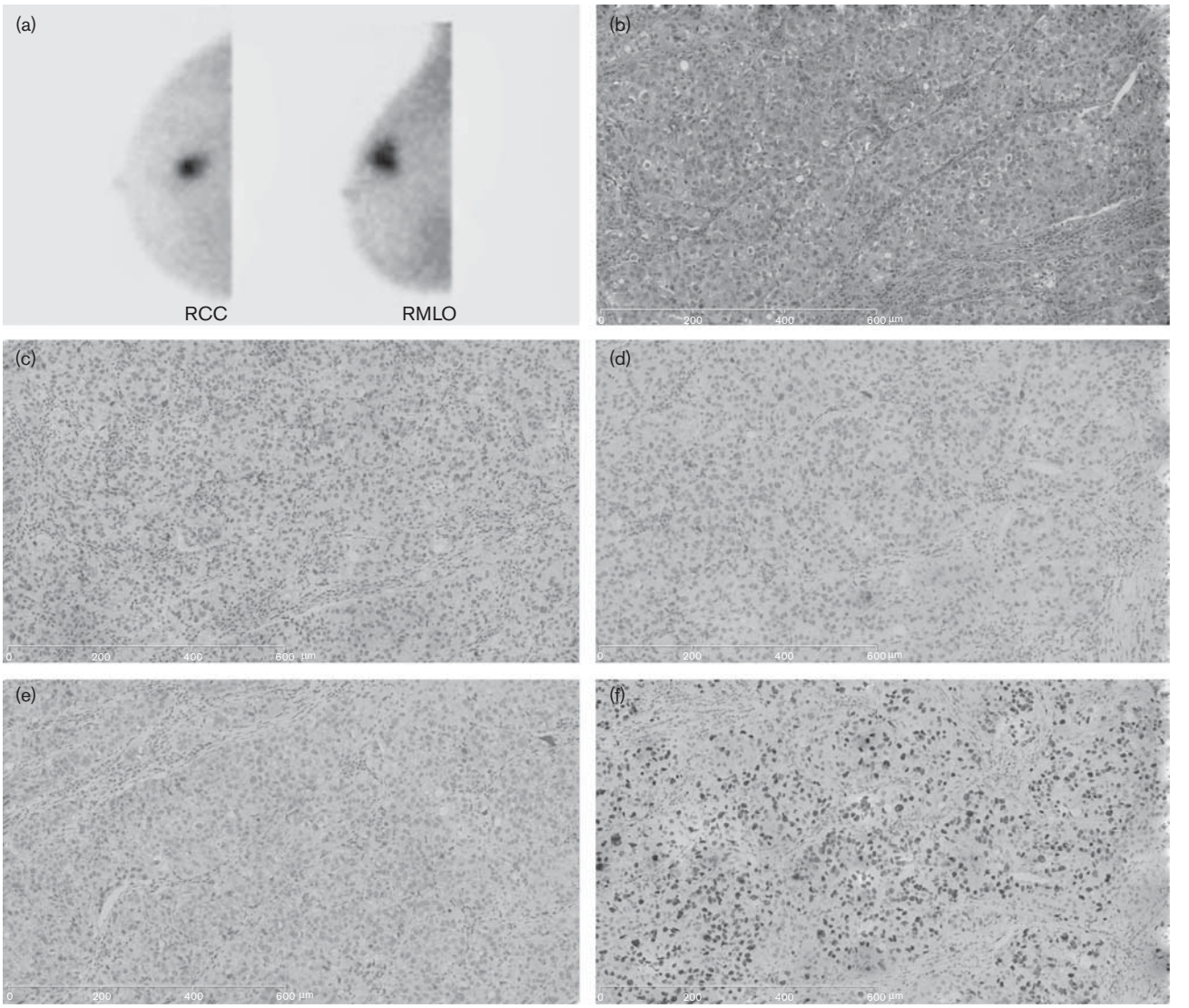

A 56-year-old woman presented with a mass in the right breast 1 week earlier. Invasive ductal carcinoma was confirmed on histologic evaluation after excision, with a tumor diameter of 2.0 cm, histologic grade III, without axillary lymph node metastasis. (a) BSGI imaging showed one round lesion with focal radioactivity uptake in the upper outer quadrant area. The values of L/N of CC and MLO were 4.47 and 3.73, respectively. The larger L/N of 4.47 was considered the semiquantitative index. (b) HE staining (×100). (c–f) Immunohistochemical staining results: (c) ER negative (×100) (d) PR negative (×100); (e) Her-2-positive staining with a score of 1+ (×100) and (f) Ki-67 more than 14% (×100). The case was grouped as triple-negative type. BSGI, breast-specific gamma imaging; CC, craniocaudal; ER, estrogen receptor; HE, hematoxylin and eosin; Her-2, human epidermal growth factor receptor 2; L/N, lesion to nonlesion ratio; MLO, mediolateral oblique; PR, progesterone receptor.

$P=0.490$), and that scored 2+ and 3+ ($t=0.910$, $P=0.370$), respectively.

Correlations between the value of L/N and molecular subtypes

Among the 102 cases, 35 out of 40 cases with Her-2 staining graded as 2+ were assessed in terms of Her-2 gene amplification by FISH, of which five cases were Her-2 positive and 30 cases were Her-2 negative. Using a combination of immunohistochemical profiles and FISH testing, there were 24 luminal A cases, 39 luminal B cases, 18 Her-2 positive cases, and 16 triple-negative breast cancers. There was no significant difference in L/N between luminal A and B ($t=0.002$, $P=1.000$), between luminal A and Her-2 positive ($t=0.120$, $P=0.910$), between luminal A and triple negative ($t=0.320$, $P=0.750$), luminal B and Her-2 positive ($t=0.150$, $P=0.890$), between luminal B and triple negative ($t=0.410$, $P=0.680$), or between Her-2 positive and triple negative ($t=0.610$, $P=0.550$), respectively, as shown in Table 2.

Fig. 3

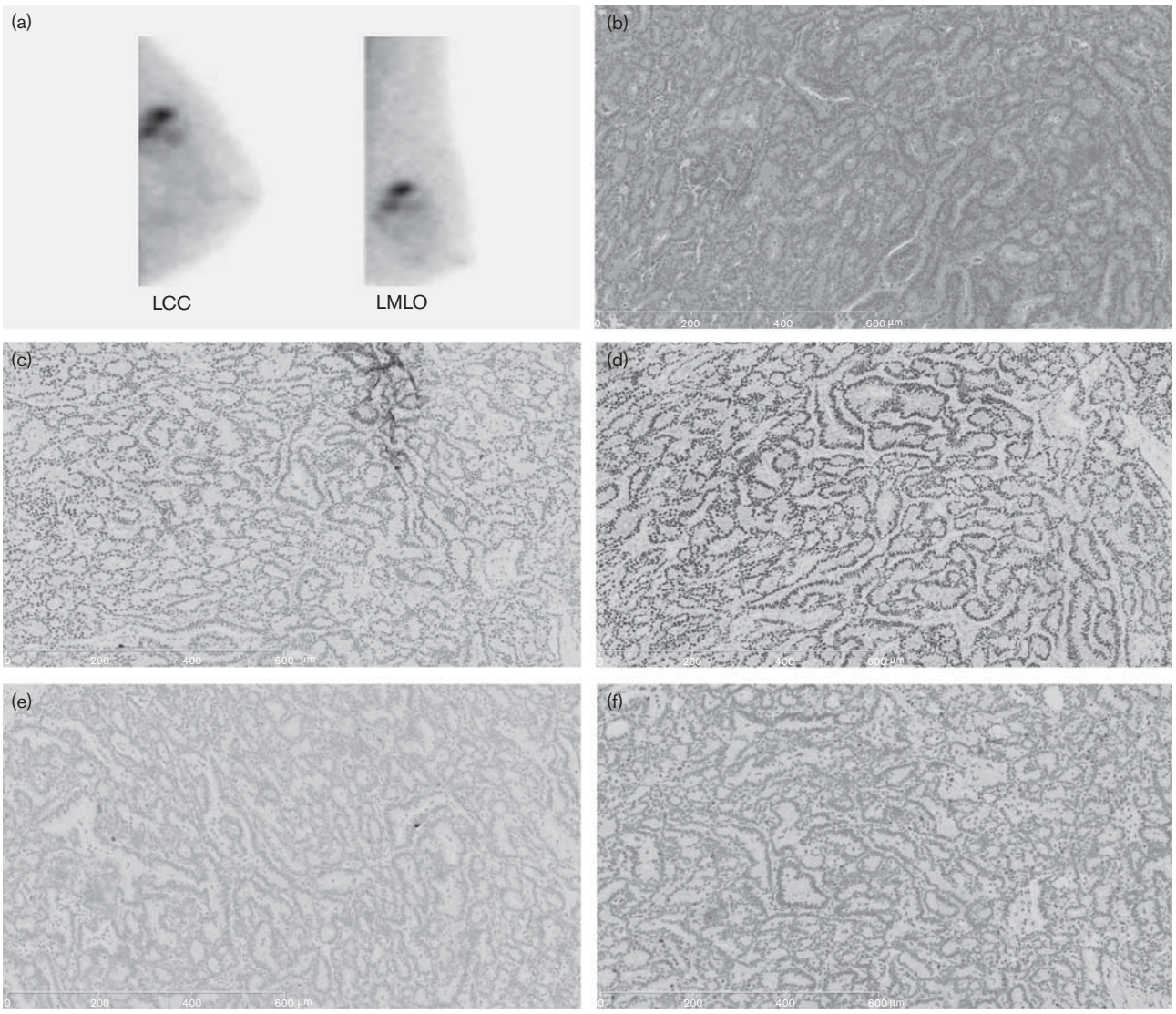

A 75-year-old woman with a left breast mass for 5 years. Intraductal papilloma with atypical hyperplasia, partly with canceration, was confirmed on pathologic inspection after excision. The tumor diameter was 2.0 cm. There was no axillary lymph node metastasis. (a) BSGI imaging indicated three lesions in the upper outer quadrant area, one with a higher focal Tc-99m-MIBI uptake than others. The values of L/N of CC and MLO were 2.82 and 3.65, respectively. The greater L/N of 3.65 was considered the semiquantitative index. (b) HE staining (×100). (c–f) Immunohistochemical staining results: (c) ER positive (×100); (d) PR positive (×100); (e) Her-2-positive staining with a score of 1 + (×100); and (f) Ki-67 less than 14% (×100). The case was grouped as luminal A type. BSGI, breast-specific gamma imaging; CC, craniocaudal; ER, estrogen receptor; HE, hematoxylin and eosin; Her-2, human epidermal growth factor receptor 2; L/N, lesion to nonlesion ratio; MLO, mediolateral oblique; PR, progesterone receptor; Tc-99m-MIBI, technetium-99m sestamibi.

Correlations between the value of L/N and clinicopathologic characteristics

The potential association between the value of L/N and breast cancer histologic grade I could not be assessed as only two breast cancer cases with grade I were present in our cohort. The value of L/N was statistically related to certain clinicopathologic characteristics including the degree of infiltration, axillary lymph node status, and tumor size (Table 2). Multivariate analysis indicated that the value of L/N was correlated positively with infiltration degree ($P = 0.016$) and tumor size ($P = 0.002$), shown in Table 3. The value of L/N between histologic grades II and III failed to reach statistical significance.

Discussion

BSGI was a useful functional technique, with a high sensitivity of 83–100% for detecting breast cancer as reported in recent studies [7,18–20]. In our study, the sensitivity of 94.1% for BSGI diagnosing breast cancer by visual analysis was similar to the reported results.

Table 2 Patient characteristics and the value of L/N

	$N=102$ [n (%)]	Value of L/N	t-test
ER status			
Negative	34 (33.3)	2.93±0.14	$t=0.330$, $P=0.740$
Positive	68 (66.7)	3.02±0.17	
PR status			
Negative	41 (40.2)	3.12±0.19	$t=0.910$, $P=0.370$
Positive	61 (59.8)	2.90±0.16	
Her-2 status			
0 and 1+	38 (37.3)	2.76±0.19	$P>0.05$
2+	40 (39.2)	3.24±0.24	
3+	24 (23.5)	2.94±0.14	
Ki-67 status (%)			
<14	34 (33.3)	2.95±0.28	$t=0.190$, $P=0.850$
≥14	68 (66.7)	3.00±0.12	
Subtype (97 cases)			
Luminal A	24 (24.7)	2.97±0.30	$P>0.05$
Luminal B	39 (40.2)	2.97±0.18	
Her-2 positive	18 (18.6)	3.01±0.19	
Triple negative	16 (16.5)	2.84±0.22	
Infiltration degree			
Noninvasive	18 (17.6)	2.25±0.14	$t=2.890$, $P=0.005$
Invasive	84 (82.4)	3.15±0.14	
Histological grade (78 cases)			
I	2 (2.1)		$t=0.240$, $P=0.810$
II	30 (31.6)	3.07±0.15	
III	46 (48.4)	3.12±0.17	
Lymph node status			
Negative	34 (33.3)	2.80±0.12	$t=2.220$, $P=0.029$
Positive	68 (66.7)	3.36±0.27	
Tumor size (cm)			
≤2	55 (53.9)	2.64±0.13	$t=3.250$, $P=0.002$
>2	47 (46.1)	3.40±0.21	

ER, estrogen receptor; Her-2, human epidermal growth factor receptor 2; L/N, lesion to nonlesion ratio; PR, progesterone receptor.

We further showed that the sensitivity of BSGI in diagnosing breast cancer was related to tumor size: 100% for cancers size more than 2.0 cm and 89.1% for less than or equal to 2.0 cm. The sensitivity of BSGI for breast cancer was higher than that of US (84.2%) and MMG (84.5%). Moreover, missed cases by US or MMG, including six breast cancer cases with dense breast tissue, were accurately diagnosed by BSGI. Therefore, our study showed that BSGI improved the sensitivity of breast cancer diagnosis, and was a useful complementary technique to US and MMG.

BSGI images, according to the 2010 guideline of Society of Nuclear Medicine and Molecular Imaging, can be analyzed and interpreted visually; however, visual analysis alone is rather subjective and remains reader dependent, particularly in terms of differentiating between likely benign and malignant lesions. Therefore, we have attempted to use an additional method, namely, the semiquantitative analysis of L/N, to aid the interpretation of BSGI images [6] and to objectively analyze related factors of Tc-99m-MIBI uptake.

Several studies have investigated the correlation between Tc-99m-MIBI uptake on scintimammography and ER, PR, Her-2, and Ki-67 status [12,13,21]. Cwikla *et al.* [12] reported that patients with PR-negative or ER-negative cancers had higher Tc-99m-MIBI uptake on scintimammography. Bonazzi *et al.* [13] reported that the value of L/N on scintimammography was correlated with the expression of Ki-67. However, other studies have shown no statistical relationship between the presence of biologic markers (ER, PR, Her-2, and Ki-67) and the value of L/N on scintimammography [21]. Although BSGI and scintimammography are both based on the same mechanisms of Tc-99m-MIBI accumulation in tumors, the equipment, the imaging time after injection of radiopharmaceuticals, the dose of Tc-99m-MIBI, and the method for determining the ROI for the semiquantitative index are different. Therefore, a dedicated investigation to assess the relationship between key BSGI and biologic markers was needed. In the present study, we found no significant correlation between the value of L/N on BSGI and ER, PR, Her-2, and Ki-67 as biologic markers. Thus, our findings support the contention that Tc-99m-MIBI accumulation in tumor cells on BSGI cannot reflect biologic profiles of breast cancer.

On the basis of the expression of those markers and the result of FISH analysis, breast cancer has been divided into four subtypes, namely, luminal A, luminal B, Her-2 positive, and triple negative, by the expert panel at the 12th International Breast Cancer Conference, St Gallen, 2011 [22]. Subtyping has been considered the essential foundation for the clinical management of breast cancer [23,24]. It is not known whether there is an association between the uptake of Tc-99m-MIBI on BSGI and subtypes of breast cancer. Some studies have suggested that the uptake fluorine-18 fluorodeoxyglucose (^{18}F-FDG) on PET imaging is correlated with different subtypes [25–27]. Here, we found no statistical difference between Tc-99m-MIBI uptake on BSGI in the different subtypes of breast cancer. This may be explained by the different mechanisms of Tc-99m-MIBI and ^{18}F-FDG accumulations in tumor. Increased uptake of Tc-99m-MIBI in cancer cells, compared with that in normal breast tissue, is proportional to the neovascularization/blood volume and increased mitochondrial density in cancer cells, whereas increased ^{18}F-FDG uptake is

Table 3 Results of multiple analysis

Variable	Unstandardized β-coefficients	SE	Standardized β-coefficients	t-value	P-value
Axillary lymph node status	0.287	0.254	0.110	1.132	0.260
Infiltration degree	0.763	0.312	0.237	2.445	0.016
Tumor size	0.726	0.227	0.294	3.204	0.002

Dependent variable: semiquantitative index of lesion to nonlesion ratio.

mainly related to increased glucose metabolism associated with malignancy.

It is well established that the clinicopathologic characteristics of a tumor (such as infiltration degree, histologic grade, axillary lymph node status, and tumor size) relate to breast cancer behavior. Some studies [12,28] have shown that Tc-99m-MIBI uptake on scintimammography was closely correlated with certain tumor clinicopathologic characteristics. In contrast, Papantoniou *et al*. [29] reported that uptake of Tc-99m-MIBI on scintimammography was not statistically different between grades II and III cancers. In this study, we found no correlation between the mean value of L/N and the histologic grades (II and III) on the BSGI. The uptake of Tc-99m-MIBI on BSGI was positively related to the degree of infiltration, tumor size, and axillary lymph node status (reflecting the higher number of metabolically active breast cancer cells). Multivariate analysis indicated that the semiquantitative index of L/N was only associated with the degree of infiltration and tumor size, not with axillary lymph node status. This may have been because axillary lymph node status has a much stronger correlation with tumor size.

There were several limitations to our study. First, our study was restricted to a single center. Second, only positive breast cancer patients were enrolled; thus, the specificity of the BSGI for breast cancer cannot be assessed. Third, the correlation of Tc-99m-MIBI uptake with outcome or survival was not assessed because of the relatively short follow-up duration in the study.

Conclusion

We found that the sensitivity of BSGI in diagnosing breast cancer by visual analysis was 94.1%, higher than that of US and MMG. Our data showed that Tc-99m-MIBI uptake in breast cancer on BSGI is associated with infiltration degree and tumor size, but not with the expression of tumor markers, histologic types, and grades.

Acknowledgements

Conflicts of interest

There are no conflicts of interest.

References

1 Rosenberg RD, Hunt WC, Williamson MR, Gilliland FD, Wiest PW, Kelsey CA, *et al*. Effects of age, breast density, ethnicity, and estrogen replacement therapy on screening mammographic sensitivity and cancer stage at diagnosis: review of 183 134 screening mammograms in Albuquerque, New Mexico. *Radiology* 1998; **209**:511–518.

2 Kolb TM, Lichy J, Newhouse JH. Comparison of the performance of screening mammography, physical examination, and breast US and evaluation of factors that influence them: an analysis of 27 825 patient evaluations. *Radiology* 2002; **225**:165–175.

3 Berg WA, Gutierrez L, NessAiver MS, Carter WB, Bhargavan M, Lewis RS, Ioffe OB. Diagnostic accuracy of mammography, clinical examination, US, and MR imaging in preoperative assessment of breast cancer. *Radiology* 2004; **233**:830–849.

4 Berg WA, Blume JD, Cormack JB, Mendelson EB, Lehrer D, Böhm-Vélez M, *et al*. Combined screening with ultrasound and mammography vs mammography alone in women at elevated risk of breast cancer. *JAMA* 2008; **299**:2151–2163.

5 Johnson N, Sorenson L, Bennetts L, Winter K, Bryn S, Johnson W, *et al*. Breast-specific gamma imaging is a cost effective and efficacious imaging modality when compared with MRI. *Am J Surg* 2014; **207**:698–701.

6 Tan H, Jiang L, Gu Y, Xiu Y, Han L, Wu P, *et al*. Visual and semi-quantitative analyses of dual-phase breast-specific gamma imaging with Tc-99m-sestamibi in detecting primary breast cancer. *Ann Nucl Med* 2014; **28**:17–24.

7 Rechtman LR, Lenihan MJ, Lieberman JH, Teal CB, Torrente J, Rapelyea JA, Brem RF. Breast-specific gamma imaging for the detection of breast cancer in dense versus nondense breasts. *Am J Roentgenol* 2014; **202**:293–298.

8 Azizun-Nisa, Bhurgri Y, Raza F, Kayani N. Comparison of ER, PR and HER-2/neu(C-erbB 2) reactivity pattern with histologic grade, tumor size and lymph node status in breast cancer. *Asian Pac J Cancer Prev* 2008; **9**:553–556.

9 Hussein MR, Abd-Elwahed SR, Abdulwahed AR. Alterations of estrogen receptors, progesterone receptors and c-erbB2 oncogene protein expression in ductal carcinomas of the breast. *Cell Biol Int* 2008; **32**:698–707.

10 Liu C, Zhang H, Shuang C, Lu Y, Jin F, Xu H, Lu P. Alterations of ER, PR, HER-2/neu, and P53 protein expression in ductal breast carcinomas and clinical implications. *Med Oncol* 2010; **27**:747–752.

11 Kim KJ, Huh SJ, Yang JH, Park W, Nam SJ, Kim JH, *et al*. Treatment results and prognostic factors of early breast cancer treated with a breast conserving operation and radiotherapy. *Jpn J Clin Oncol* 2005; **35**:126–133.

12 Cwikla JB, Buscombe JR, Kolasinska AD, Parbhoo SP, Thakrar DS, Hilson AJ. Correlation between uptake of Tc-99m sestaMIBI and prognostic factors of breast cancer. *Anticancer Res* 1999; **19** (3B):2299–2304.

13 Bonazzi G, Cistaro A, Bellò M, Bessone M, Tetti M, Villata E, *et al*. Breast cancer cellular proliferation indexes and ^{99m}Tc-sesta MIBI capture: what correlation? *J Exp Clin Cancer Res* 2001; **20**:91–94.

14 Park JY, Yi SY, Park HJ, Kim MS, Kwon HJ, Park NH, Moon SY. Breast-specific gamma imaging: correlations with mammographic and clinicopathologic characteristics of breast cancer. *Am J Roentgenol* 2014; **203**:223–228.

15 Goldsmith SJ, Parsons W, Guiberteau MJ, Stern LH, Lanzkowsky L, Weigert J, *et al*. SNM practice guideline for breast scintigraphy with breast-specific gamma-cameras 1.0. *J Nucl Med Technol* 2010; **38**:219–224.

16 Park KS, Chung HW, Yoo YB, Yang JH, Choi N, So Y. Complementary role of semiquantitative analysis of breast-specific gamma imaging in the diagnosis of breast cancer. *Am J Roentgenol* 2014; **202**:690–695.

17 Hammond ME, Hayes DF, Wolff AC, Mangu PB, Temin S. American Society of Clinical Oncology/College of American Pathologists guideline recommendations for immunohistochemical testing of estrogen and progesterone receptors in breast cancer. *J Oncol Pract* 2010; **6**:195–197.

18 Weigert JM, Bertrand ML, Lanzkowsky L, Stern LH, Kieper DA. Results of a multicenter patient registry to determine the clinical impact of breast-specific gamma imaging, a molecular breast imaging technique. *Am J Roentgenol* 2012; **198**:69–75.

19 Lee A, Chang J, Lim W, Kim BS, Lee JE, Cha ES, Moon BI. Effectiveness of breast-specific gamma imaging (BSGI) for breast cancer in Korea: a comparative study. *Breast J* 2012; **18**:453–458.

20 Sun Y, Wei W, Yang HW, Liu JL. Clinical usefulness of breast-specific gamma imaging as an adjunct modality to mammography for diagnosis of breast cancer: a systemic review and meta-analysis. *Eur J Nucl Med Mol Imaging* 2013; **40**:450–463.

21 Papantoniou VJ, Souvatzoglou MA, Valotassiou VJ, Louvrou AN, Ambela C, Koutsikos J, *et al*. Relationship of cell proliferation (Ki-67) to ^{99m}Tc-(V)DMSA uptake in breast cancer. *Breast Cancer Res* 2004; **6**:56–62.

22 Goldhirsch A, Wood WC, Coates AS, Gelber RD, Thürlimann B, Senn HJ. Panel members. Strategies for subtypes – dealing with the diversity of breast cancer: highlights of the St. Gallen International Expert Consensus on the Primary Therapy of Early Breast Cancer 2011. *Ann Oncol* 2011; **22**:1736–1747.

23 García Fernández A, Chabrera C, García Font M, Fraile M, Gónzalez S, Barco I, *et al*. Differential survival and recurrence patterns of patients operated for breast cancer according to the new immunohistochemical classification: analytical survey from 1997 to 2012. *Tumour Biol* 2013; **34**:2349–2355.

24 García Fernández A, Giménez N, Fraile M, González S, Chabrera C, Torras M, *et al*. Survival and clinicopathological characteristics of breast cancer patient according to different tumour subtypes as determined by hormone receptor and Her2 immunohistochemistry. a single institution survey spanning 1998 to 2010. *Breast* 2012; **21**:366–373.

25 Koo HR, Park JS, Kang KW, Cho N, Chang JM, Bae MS, *et al.* ^{18}F-FDG uptake in breast cancer correlates with immunohistochemically defined subtypes. *Eur Radiol* 2014; **24**:610–618.
26 Gilardi L, Colleoni M, Paganelli G. PET/CT and breast cancer subtypes. *Eur J Nucl Med Mol Imaging* 2013; **40**:1301–1303.
27 García Vicente AM, Soriano Castrejón Á, León Martín A, Chacón López-Muñiz I, Muñoz Madero V, Muñoz Sánchez Mdel M, *et al.* Molecular subtypes of breast cancer: metabolic correlation with ^{18}F-FDG PET/CT. *Eur J Nucl Med Mol Imaging* 2013; **40**:1304–1311.
28 Tadwalkar RV, Rapelyea JA, Torrente J, Rechtman LR, Teal CB, McSwain AP, *et al*. Breast-specific gamma imaging as an adjunct modality for the diagnosis of invasive breast cancer with correlation to tumour size and grade. *Br J Radiol* 2012; **85**:212–216.
29 Papantoniou V, Christodoulidou J, Papadaki E, Valotassiou V, Souvatzoglou M, Louvrou A, *et al.* Uptake and washout of ^{99m}TcV-dimercaptosuccinic acid and ^{99m}Tc-sestamibi in the assessment of histological type and grade in breast cancer. *Nucl Med Commun* 2002; **23**:461–467.